# EPR Mapping of Interactions between Spin-Labeled Variants of Human Carbonic Anhydrase II and GroEL: Evidence for Increased Flexibility of the Hydrophobic Core by the Interaction†

Malin Persson,‡ Per Hammarström,‡ Mikael Lindgren,§ Bengt-Harald Jonsson,|| Magdalena Svensson,‡ and Uno Carlsson*,‡

*IFM-Departments of Chemistry and of Chemical Physics, Linköping University, S-581 83 Linköping, Sweden, and Department of Biochemistry, Umeå University, S-901 87 Umeå, Sweden*

*Received June 17, 1998; Revised Manuscript Received October 19, 1998*

ABSTRACT: Human carbonic anhydrase II (HCA II) interacts weakly with GroEL at room temperature. To further investigate this interaction we used electron paramagnetic resonance (EPR) spectroscopy to study HCA II cysteine mutants spin-labeled at selected positions. From our results it is evident that protein−protein interactions can be specifically mapped by site-directed spin-labeling and EPR measurements. HCA II needs to be unfolded to about the same extent as a GuHCl-induced molten-globule intermediate of the enzyme to interact with GroEL. The interaction with GroEL includes interactions with outer parts of the HCA II molecule, such as peripheral $\beta$-strands and the N-terminal domain, which have previously been shown to be rather unstable. As a result of the interaction, the rigid and compact hydrophobic core exhibits higher flexibility than in the molten globule, which is likely to facilitate rearrangements of misfolded structure during the folding process. The degree of binding to GroEL and accompanying inactivation of the enzyme depend on the stability of the HCA II variant, and nonspecific hydrophobic interactions appear to be most important in stabilizing the GroEL−substrate complex.

It has, for some time, been known that special cellular proteins, called chaperones, exist and that they protect other proteins from aggregation when a cell is exposed to elevated temperatures and stress. It is generally believed that chaperones interact with non-native proteins exposing hydrophobic surfaces and assist in protein folding or maintain proteins in an extended conformation for transport through membranes (*1*−*3*). The most thoroughly studied chaperone is the chaperonin GroEL and its co-chaperonin GroES, which are found in *Escherichia coli* (*4*). The mechanism by which the GroEL−GroES complex binds and releases substrate proteins is still not completely understood (*5*).

One of the most challenging questions to be answered concerns how GroEL exerts its protective action: whether it is a passive, that is, functions as a test tube (*6*), or an active process, that is, functions as an unfoldase (*7*), what kind of interactions are important, and how the conformation of the bound protein is affected by GroEL. The crystal structures of GroEL and the GroEL−GroES complex have recently been determined (*8*−*10*). The GroEL protein is a tetradecamer comprising identical subunits that are arranged in a double heptameric ring structure. The GroEL complex forms a cylindrical cavity in which the presumed protein substrate-binding site has been localized to the inside surface of the apical domain of each of the subunits. This area consists mainly of hydrophobic amino acid residues, which indicates the importance of hydrophobic interactions in the binding of protein substrates (*11*, *12*). In addition, folding studies on a variety of proteins have shown that the binding of the substrate protein to GroEL is probably due to hydrophobic interactions (*11*−*20*), although charged interactions might be essential in some cases (*18*, *20*−*22*). Moreover, there is evidence that GroEL actively unfolds the protein substrate, thereby giving the protein a new opportunity to fold correctly (*16*, *23*−*25*).

We have previously demonstrated that human carbonic anhydrase II (HCA II)[1] interacts rather weakly with GroEL at room temperature (*26*) and that the amount of HCA II bound to GroEL increases significantly at elevated temperatures (*27*, *28*). We have also noted that GroEL lowers the apparent activation energy for the refolding of HCA II (*28*), suggesting that GroEL has a substantial influence on the folding pathway.

To further investigate and map the interactions between GroEL and HCA II, we initiated a study on cysteine mutants

† This work was supported by grants from the Swedish National Board for Industrial and Technical Development (U.C., B.-H.J.), the Swedish Natural Science Research Council (U.C., B.-H.J., M.L.), "Knut och Alice Wallenbergs Minnesfond" (M.L.), "Stiftelsen Bengt Lundqvists Minne" (M.P.), "Marcus och Amalia Wallenberg Minnesfond" (M.P., U.C.), "Carl Tryggers Stiftelse för Vetenskaplig Forskning" (M.L.).

* To whom correspondence should be addressed. Tel: (+46) 13 281714. Fax: (+46) 13 281399. E-mail: ucn@ifm.liu.se.

‡ IFM-Department of Chemistry, Linköping University.

§ IFM-Department of Chemical Physics, Linköping University.

|| Umeå University.

[1] Abbreviations: EPR, electron paramagnetic resonance; GuHCl, guanidine hydrochloride; HCA II, human carbonic anhydrase II; spin-HCA II, spin-labeled HCA II; spin-W97C, spin-labeled Cys-97 in a Trp-97 → Cys mutant of HCA II (other spin-labeled mutants are abbreviated analogously).

10.1021/bi981442e CCC: $18.00 
Published on Web 12/08/1998

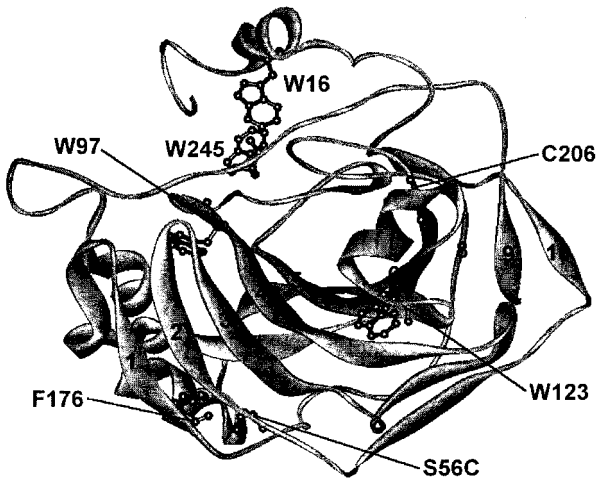


FIGURE 1: Cartoon of HCA II with mutated and spin-labeled cysteine positions indicated. The 3D structure is based on the crystal structure determined by Håkansson et al. (*34*).

of HCA II that were specifically labeled with a spin-probe (nitroxide radical) at different positions in both the interior and the exterior parts of the native protein structure (Figure 1). These spin-labeled mutants were thoroughly characterized by EPR spectroscopy in our earlier studies of HCA II folding (*29*−*31*). Site-directed spin-labeling has also been used by other researchers to investigate the interaction between the chaperone α-crystallin and substrate peptides (*32*).

HCA II has a molecular weight of 29 300, and its structure is well-characterized (*33*, *34*). The protein consists of a dominating $\beta$-sheet made up of 10 $\beta$-strands, and that sheet divides the molecule into two halves (Figure 1). Each half contains a hydrophobic cluster, that is, there is one in the N-terminal region and a larger one in the main domain. The active site is located in a conical cavity that penetrates about 15 Å into the middle of the main domain between $\beta$-strands 4 and 5 (Figure 1). The folding behavior of HCA II has been extensively studied (*35*), and it has been shown that the unfolding of the protein is a three-stage process including the formation of a stable equilibrium intermediate of molten-globule-type (*36*). The central part of the large $\beta$-core is extremely stable and retains a compact nativelike structure under very strong denaturing conditions (*31*, *36*, *37*).

In earlier studies of HCA II, we found that the mobility of the spin-label, as determined from the EPR line-shape, can give detailed information about structural and conformational changes during various stages of the folding process. In the present investigation we used a similar approach to elucidate the structural changes that accompany the temperature-dependent interaction between GroEL and HCA II. The increased temperature leads to a partially unfolded structure of HCA II with the EPR line-shape of the spin-label reflecting local motions of the more flexible side chains. Relative changes of the mobility of spin-labels in different positions in HCA II upon binding to GroEL, in terms of line-broadening or line-sharpening of the associated EPR spectral lines, are demonstrated and discussed.

## MATERIALS AND METHODS

*Chemicals*. The spin-label *N*-(1-oxyl-2,2,5,5-tetramethyl-3-pyrrolidinyl)iodoacetamide was purchased from Sigma. All other chemicals were of reagent grade.

*Spectrophotometers*. Light absorbance measurements for protein concentration determinations were performed on a Hitachi U2000 spectrophotometer. Fluorescence was measured on a Hitachi F-4500 spectrofluorimeter for the $T_m$ value determinations.

*Protein Isolation and Purification*. HCA II and mutants thereof were expressed in *E. coli* and were purified by affinity chromatography, as described earlier (*36*). GroEL was prepared as described earlier (*26*, *27*) with an additional incubation of GroEL with GroES and ATP, followed by gel filtration as described by Mitzobata et al. (*38*) to further purify GroEL from the nonspecific association of different peptides. The absence of tryptophan in the purified GroEL was shown by fluorescence measurements (*39*, *40*). The concentration of GroEL was determined according to the Bio-Rad protein assay (*41*).

*Spin-Labeling*. The modification of SH groups with the spin-label was performed as previously described (*29*, *31*).

*Preparation of Samples for EPR and Inactivation*−*Reactivation Measurements*. The samples for EPR and activity measurements were prepared as follows: 8.5 $\mu$M spin-labeled HCA II was mixed in the incubation buffer, 0.1 M Tris-$H_2SO_4$, pH 7.5, containing 0.2 M GuHCl, and, when indicated, equimolar amounts of GroEL were added as well. All stock solutions of GroEL and spin-labeled HCA II used in the experiments were initially buffered in 0.1 M Tris-$H_2SO_4$, pH 7.5, so as to avoid the dilution of the buffer in the various reactivation experiments.

*Inactivation and Reactivation of Spin-Labeled HCA II with and without GroEL*. The inactivation of spin-labeled HCA II without GroEL was initiated by adding spin-labeled HCA II to the incubation buffer equilibrated to the temperature of the measurement. The inactivation of spin-labeled HCA II with GroEL was initiated by adding spin-labeled HCA II and GroEL simultaneously to the same buffer as that above. The activity was monitored by the $CO_2$ hydration assay described elsewhere (*42*, *43*) and measured as a function of time until equilibrium was reached between active and inactive enzyme.

The reactivation experiments of heat-denatured spin-labeled HCA II were performed as described elsewhere (*27*) for the unlabeled protein. In short, the samples were prepared as indicated above and were then incubated for 1 h at 50 °C; thereafter the temperature was lowered to 20 °C. To monitor the reactivation we measured the activity as a function of time until equilibrium between active and inactive HCA II was reached.

*EPR Measurements*. EPR measurements were carried out using a Bruker ER200D-SRC CW EPR spectrometer. An ER4102TM cavity with its standard variable temperature insert was used, and samples were inserted in the appropriate flat sample cells (Wilmad & Co). A Bruker VT4112 system was used to measure the temperature. We found it necessary to calibrate the temperature at the position of the sample in the cell by using an external thermocouple, because the sample temperature is sensitive to both the heater and the flow of nitrogen gas. To minimize the negative effects of diffusion in and out of the active sample region in the cavity, we filled only the lower portion of the sample cell with protein solution. It took approximately 4−5 min for the temperature to change between 20 and 50 °C at the position of the sample within the variable temperature holder. The

time when reaching this temperature was set to 0 when monitoring time-dependent changes. It was judged that another two to three minutes was required to equilibrate the temperature of the sample within the (semi-) filled cell. The scan time was always the same: 4.5 min.

The samples of spin-labeled HCA II, as well as mixtures of spin-labeled HCA II and GroEL, were also investigated with respect to time-dependent changes before, during, and after incubation took place. Typically, a mixture of spin-labeled HCA II and GroEL was inserted in an EPR sample cell at 20 °C and spectra were recorded as a function of time. This process was usually allowed to continue for 30−45 min in order to investigate possible complex formation already at room temperature. Thereafter the temperature was raised to 50 °C and spectra were recorded as a function of time for about 1 h to ensure that equilibrium was reached. After the heat incubation, the temperature was lowered to 20 °C and spectra were recorded as a function of time for 2 h. The procedure described above was repeated for at least two series of samples of different origin.

*Processing of Experimental EPR Data*. Although all of the integrated EPR spectra (with the exception of those associated with heat-treated samples in the absence of GroEL) showed only minor variations in terms of integrated EPR signal intensity, the presented EPR spectra have all been baseline corrected and normalized to a constant spin concentration (Bruker Win-EPR ver. 2.11 and Matlab 5.1). Thus, a line width change can also be interpreted as a difference in the associated spectral amplitudes.

*Determination of $T_m$*. Spin-labeled protein was added to the incubation buffer (see above) to a concentration of 0.5 $\mu$M. A 1-mL aliquot of the sample was filtered through a 0.45-$\mu$m filter (Millipore) into the sample cuvette. The cuvette was placed in a circulating water bath for effective heating. The temperature was varied stepwise (2−5 °C) in the range 10−65 °C, depending on the stability of the mutant. After reaching a selected temperature, the sample was incubated for 15 min prior to the measurement. The cuvette was rapidly placed in a thermostated cell holder in the spectrofluorimeter, and three accumulative fluorescence spectra were recorded in the wavelength range 315−450 nm with an excitation wavelength of 295 nm, using 5 nm emission and 10 nm excitation slits except when studying the spin-W16C and spin-W97C mutants, for which 10 nm slits were used for both emission and excitation. After correction with the appropriate blank, each emission peak was analyzed through first derivative calculation to find the emission maximum. The $T_m$ value was calculated as described elsewhere (*44*).

As a control experiment $T_m$ of HCAII was also determined by differential scanning calorimetry (Microcal MC-2). The protein concentration was 34 $\mu$M, and the scan rate was 1 °C/min.

## RESULTS AND DISCUSSION

*Heat-Induced Unfolding of the Spin-Labeled HCA II Mutants*. We have previously shown that GroEL has the capability to protect HCA II from irreversible aggregation at elevated temperatures. This leads to high yields of active enzyme when the temperature is lowered, despite a rather weak interaction between the chaperonin GroEL and HCA II at room temperature (*26*, *27*). The chaperoning activity of GroEL seems to be accomplished by reversible binding of an inactive form of HCA II that is capable of reactivation. Thus, unfolded forms of HCA II resulting from the heat treatment are interacting with GroEL, and it should therefore be possible to map the extent of this interaction specifically by site-directed spin-labeling of the target molecule, HCA II.

Table 1: Inactivation, Reactivation, and $T_m$ of Spin-Labeled Variants of HCA II

| | activity[a] (%) | | | | |
|---|---|---|---|---|---|
| spin-labeled variant | without GroEL, without heating | after heating[c] | with GroEL, without heating | after heating[d] | $T_m$ value (°C)[b] |
| C206 | 95 | 20 | 85 | 75 | 35 |
| W16C | 92 | 50 | 75 | 75 | 36 |
| S56C | 90 | 10 | 30 | 20 | 32 |
| W97C | 85 | 2 | 40 | 40 | 31 |
| W123C | 95 | 6 | 58 | 58 | 36 |
| F176C | 98 | 4 | 22 | 39 | 31 |
| W245C | 95 | 23 | 93 | 80 | 39 |

[a] After 4 h of incubation in 0.2 M GuHCl at 20 °C. [b] Determined from fluorescence measurements. [c] The spin-labeled variants were incubated for 1 h at 50 °C before incubation at 20 °C. [d] The spin-labeled variants were together with GroEL incubated for 1 h at 50 °C before incubation at 20 °C.

$T_m$ values of the spin-labeled HCA II variants were determined in the reactivation buffer to study the effects of spin-labeling on stability and to determine resistance to heat denaturation. The unfolding induced by heating was monitored by the red shift of the intrinsic Trp fluorescence spectrum. This parameter reflects the global unfolding of HCA II, since the 7 Trp residues of the protein are distributed in the molecule. Previously, we have also shown that the determination of the stability of all possible single-point Trp mutants of HCAII can be done independently of the method used (fluorescence, UV absorbance, or enzyme activity), strongly indicating that different Trp content does not interfere with the obtained stability data (*45*, *46*).

The determined $T_m$ values were further validated by a control experiment on unmutated HCAII using a differential scanning calorimeter (DSC). The $T_m$ values obtained from the DSC and fluorescence experiment only differed by 1 °C.

All spin-labeled variants had $T_m$ values in the temperature range 31−39 °C (Table 1) and all had reached a plateau value at 50 °C; hence, a suitable high-temperature limit for the study of GroEL and the spin-labeled variants of HCA II was 50 °C.

The fluorescence spectra of all of the spin-labeled variants were red-shifted to 342−344 nm at 50 °C, showing that the state of unfolding was similar for all of these variants. Comparisons with fluorescence spectra of GuHCl-unfolded HCA II show that these wavelength maxima correspond to an exposure of Trp residues that is observed in the molten-globule state of the protein (*45*).

Measurements on unlabeled HCA II showed that the addition of equimolar amounts of GroEL lowered the $T_m$ value by 7 °C. The temperature dependence on the reactivation yield of denatured HCA II was earlier shown to be affected in a similar way, when GroEL was present (*27*). The fluorescence spectrum of the unlabeled HCA II was red-

shifted to 341 nm after the heat unfolding transition. In the presence of GroEL, the corresponding heat transition led to a Trp fluorescence maximum at 342 nm, indicating that the tryptophans in the bound HCA II are not fully exposed. The observed red shift can be attributed only to unfolding of HCA II, because GroEL does not contain any Trp residues (*40*).

All $T_m$ experiments were performed in buffers containing 0.2 M GuHCl, and this GuHCl addition was also included in all subsequent measurements. The rationale for performing all experiments in 0.2 M GuHCl is that, without the destabilizing effect by GuHCl, it is impossible to induce the molten-globule-like conformation at a temperature that GroEL will withstand without being heat-denatured. In the absence of GuHCl a temperature of 60−65 °C was required to complete the unfolding transition of HCA II to the molten-globule-like state, whereas only 50 °C was needed in the presence of 0.2 M GuHCl. At 60 °C no chaperone action on HCA II could be detected because GroEL was denatured at this temperature, whereas HCA II can be chaperoned at 50 °C. Another reason for running the inactivation−reactivation experiments in low concentrations of GuHCl is that previously cited GroEL-mediated refolding studies on HCA II have been performed in this medium (*26*−*28*), permitting us to make comparisons under similar conditions. It has previously been shown that the action of GroEL can be affected by GuHCl (*47*). In that study it was demonstrated that low concentrations of GuHCl decreased the ATPase activity of GroEL and destabilized the GroEL/ES complex, thus relieving the inhibition of GroEL ATPase by GroES. However, the refolding of HCA II can be efficiently assisted by GroEL without GroES and ATP. Since GroEL alone is used in this study, the known effects by GuHCl on the chaperonin should be off-set. In a control experiment both the spontaneous and the GroEL-mediated refolding behavior of HCA II were also shown to be very similar in urea (0.6 M) and GuHCl (0.2 M).

*Heat Inactivation and Reactivation with and without GroEL*. These experiments were primarily performed to see whether the spin-labeled mutants appeared to be chaperoned by GroEL in the same manner as the unlabeled and unmutated form of HCAII used in a previously published study (*27*). Thus, these experiments should be regarded primarily as verifying experiments rather than giving information on detailed mechanistic aspects of the chaperone action of GroEL on HCAII. Inactivation−reactivation experiments at different temperatures are not straightforward to interpret because temperature affects many parameters such as the stability of HCAII and GroEL, aggregation behavior, and binding strength to GroEL. At 20 °C slow inactivation of the spin-labeled mutants occurred when GroEL was present, and the time course of this process is shown in Figure 2 for a representative variant, spin-W97C. The equilibrium value of the inactivation corresponds to 40% of the remaining enzyme activity. Similar inactivation behavior was also observed at 20 °C for the rest of the spin-labeled variants, and the equilibrium values in terms of remaining activities are given in Table 1.

All of the spin-labeled HCA II variants were incubated at 50 °C for 1 h together with GroEL, and complete inactivation occurred within the first 3 min. When the temperature was subsequently lowered to 20 °C, the protein variants were all

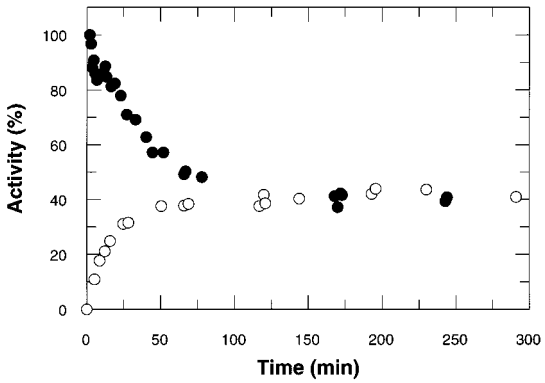


FIGURE 2: The activity of spin-W97C mutant as a function of time for (●) inactivation of spin-W97C in the presence of GroEL at 20 °C, and (○) recovery of enzyme activity of spin-W97C in the presence of GroEL at 20 °C after incubation for 1 h in 50 °C. There is no remaining enzyme activity at 50 °C.

reactivated to approximately the same level as during the inactivation experiments at 20 °C (described above). The reactivation process as a function of time is shown for spin-W97C (Figure 2), and the recovered activities for all of the spin-labeled variants after GroEL-assisted refolding are presented in Table 1. It is evident that equilibrium was attained because starting from the denatured or the native state of the spin-labeled HCA II variants led to similar levels of activity. For heat-denatured (50 °C, 1 h) spin-labeled HCA II variants, all but spin-W16C gave low yields of active enzyme upon unassisted reactivation at 20 °C (Table 1).

The results regarding inactivation and reactivation that were obtained in an earlier study of unlabeled HCA II in the presence and absence of GroEL (*27*) are very similar to the data acquired with the spin-labeled HCA II used in the present study. Therefore, it is reasonable to believe that the engineered mutations as well as the spin-labeling of HCA II have not caused structural alterations that will significantly affect the chaperone action of GroEL.

We earlier interpreted our results to say that there is an equilibrium between an inactive HCA II intermediate, probably bound to GroEL, and the active enzyme. The observed increase in the inactivation rate in the presence of GroEL was attributed to a shift in the equilibrium, away from the native state, caused by rapid binding of GroEL to the inactive intermediate.

*The Dependence of Protein Stability on the Interaction with GroEL*. An approximately linear relationship was noted for the stability of the spin-labeled variants toward heat denaturation and formation of the corresponding inactive intermediate caused by the GroEL interaction at 20 °C (Figure 3). A similar correlation between the stability and the fraction of remaining inactive intermediate was also found when the spin-labeled variants were first heat-denatured and then renatured in the presence of GroEL at 20 °C (Table 1).

*EPR Behavior of Spin-Labeled HCA II at Elevated Temperatures*. The spectra recorded at room temperature (20 °C) for the various spin-labeled HCA II variants showed the characteristic features described in our previous study (*31*). Buried sites were generally associated with a less mobile spin-label, whereas the variants with spin-label positions in the exterior parts of the molecule showed more of the characteristic three-line spectra expected for a flexible environment. The buried sites (residues 97, 123, 206) are

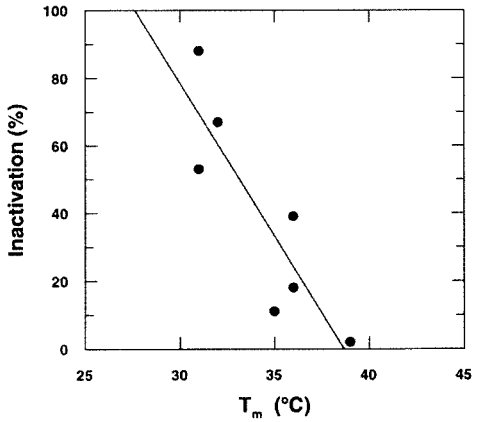


FIGURE 3: GroEL-mediated inactivation of spin-labeled variants of HCA II at 20 °C as a function of thermodynamic stability (temperature of melting, $T_m$). Inactivation data are normalized with respect to inactivation without GroEL at 20 °C (Table 1).

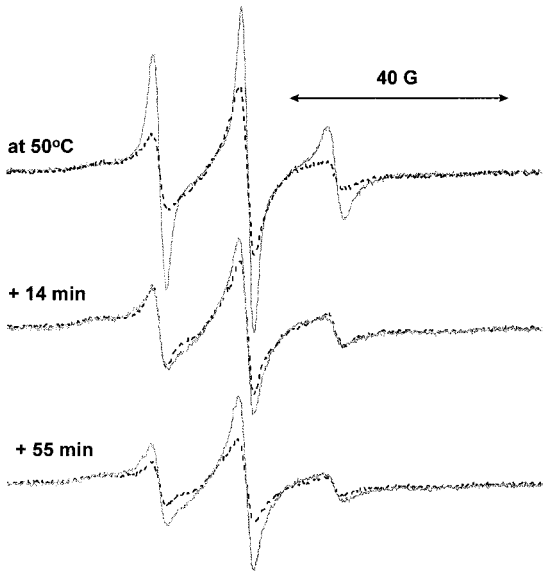


FIGURE 4: Effect of time on the EPR signal of spin-S56C during heat treatment at 50 °C with GroEL (gray spectra) and without GroEL (dashed spectra). As noted the signal remains unchanged in the presence of GroEL. The recording of the top spectrum was initiated when the sample reached 50 °C.

also those with low $B$ values (6−8 Å$^2$) from the crystal structure, whereas the more exposed sites (residues 16, 56, 176, 245) have higher $B$ values (9−12 Å$^2$) indicating a more flexible structure in the outer parts of the molecule (*34*). Upon warming of the samples, the EPR lines became progressively narrower due to the onset of thermally assisted unfolding of the protein, but this effect was essentially reversible as long as the sample temperature was held below $T_m$. At temperatures above $T_m$, the EPR lines initially became narrower but broaden after storage at these temperatures (Figure 4).

The latter process was observed for all spin-labeled HCA II variants, although the time evolution and final appearance of the broadened EPR line-shape varied. This broadening of EPR lines was associated with a precipitation in the EPR sample cell; thus we obtained both visible and spectroscopic evidence of aggregation of the unfolded spin-labeled HCA II variants at elevated temperatures. During the course of the experiment, particularly when bringing the sample

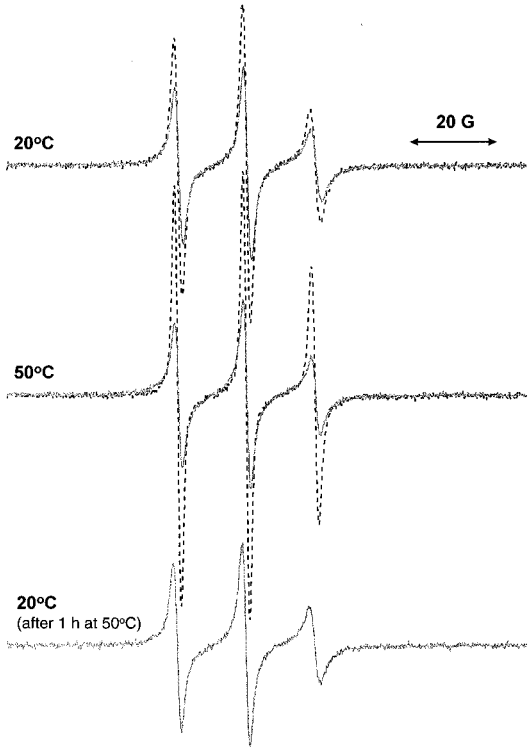


FIGURE 5: Effect of temperature on the EPR signal of spin-W16C: initially at 20 °C (top), when reaching 50 °C (middle), and after reactivation has been completed at 20 °C (lower). Reactivation: Heat-treated (1h, 50 °C) protein was cooled to 20 °C; sample with GroEL (gray spectra) and sample without GroEL (dashed spectra). All spectra (normalized) are plotted with the same amplitude scale.

temperature back to 20 °C, the precipitate tended to accumulate at the bottom of the sample cell, making further EPR quantification of these heat-treated samples unreliable. The low reactivation yields of the heat-denatured spin-labeled HCA II variants are in accordance with these observations (Table 1). When samples comprising mixtures of spin-labeled HCA II and GroEL were subjected to temperatures above $T_m$ of the spin-labeled HCA II variants (i.e., at 50 °C), no precipitate was seen, and the associated EPR spectra were unchanged over time; this behavior is illustrated for the spin-S56C mutant in Figure 4. Furthermore, the EPR spectra of spin-labeled HCA II variants in the presence of GroEL regained their original features when the temperature was brought back to room temperature after the heat treatment, which is in contrast to what happened when GroEL was not present in the sample cell. This is exemplified for spin-W16C in Figure 5. These spectral observations are supported by the inactivation−reactivation data above, which show that equilibrium was reached from both the heat-denatured and the native state of the spin-labeled HCA II variants in the presence of GroEL.

The EPR spectra of GroEL-bound spin-labeled variants were in some cases different from those of the spin-labeled variants without GroEL; these differences are presented and analyzed below.

*Interaction with the N-terminal Domain. W16C.* Position 16 is near the surface in the N-terminal part of the molecule (Figure 1). The mobility of the spin-label in that position was relatively large in the native state at 20 °C, and a broadening of the line-shape was observed in the presence

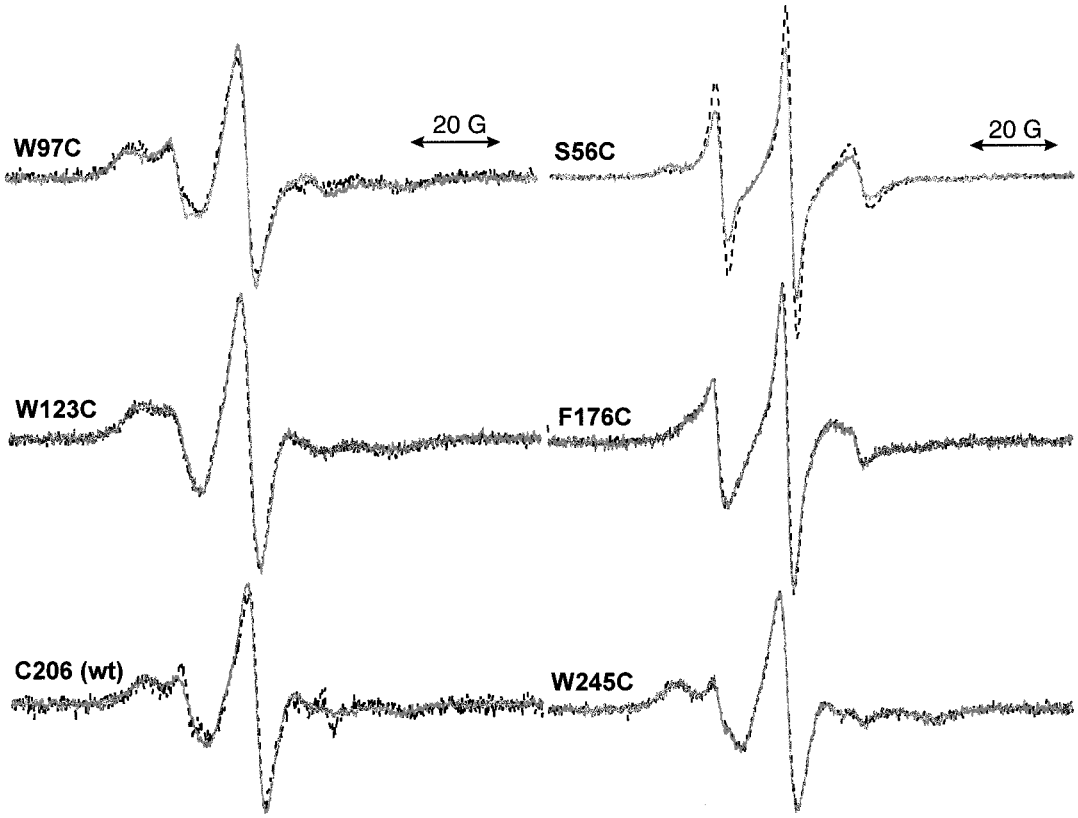


FIGURE 6: Various EPR spectra of spin-labeled variants of HCA II (indicated by insets) with (gray spectra) and without (dashed spectra) the presence of GroEL. All spectra were recorded at 20 °C. The samples with GroEL were allowed to equilibrate for 30−45 min before recording. The amplitude scale within each pair of normalized spectra is the same; however, the amplitude scale may differ among the various variants.

of GroEL together with the spin-labeled mutant, both at 20 and 50 °C (Figure 5). This indicates that there is an interaction between the substructure around position 16 and GroEL. If an interaction had not taken place, the EPR lines would have been the same in the presence and absence of GroEL.

*Interaction with the Main β-core*

*S56C.* This position is located peripherally in β-strand 2 of the main domain of the HCA II molecule (Figure 1). The mobility of the spin-label in this position was relatively large in the native state at 20 °C (Figure 6). The spectra of spin-S56C with and without GroEL were identical immediately after mixing, but as time progressed the EPR lines broadened considerably of the spin-S56C spectrum in the presence of GroEL (data not shown).

An increase in the temperature to 50 °C should result in greater mobility of the spin-label, that is, the peaks in the EPR spectra are expected to become narrower due to thermally assisted unfolding, and this was found for spin-S56C without GroEL. However, for spin-S56C in the presence of GroEL the line-shape broadening indicates lower mobility of the spin-label at 50 °C than at 20 °C (Figures 6 and 7). Thus, GroEL interacts with a larger population of spin-S56C molecules at 50 °C than at 20 °C. At 50 °C the amplitude of spin-S56C spectra in the absence of GroEL decreased gradually with time, whereas the spectra in the presence of GroEL appeared unchanged (Figure 4). This was due to aggregation in the absence of GroEL, which is corroborated by a visible precipitate within the sample cell as discussed in a previous subsection.

Lowering the temperature of the GroEL-containing sample again to 20 °C (after the heat treatment) the EPR signal became broader, since the viscosity increases and a large population of the protein substrate is still bound to GroEL. However, the signal changes toward the same line-shape as was noted in the EPR spectrum of spin-S56C in the presence of GroEL before heat treatment. The phenomenon is illustrated in Figure 8, showing the EPR spectra associated with the initial and final states of this process. Analysis of the reactivation kinetics yielded a half-life of 23 min. A similar time constant could be estimated from the changes of EPR spectra; however, since the amplitude changes were rather small the obtained values are too uncertain to give accurate kinetic information.

*W97C.* This amino acid is located in β-strand 4 and is part of the stable hydrophobic cluster in HCA II (Figure 1). Solvent accessibility studies have shown that position 97 is deeply buried inside the HCA II molecule (*33*), and chemical labeling data indicate that the substructure around this position, which comprises β-strands 3−5, is remarkably stable, retaining a compact residual structure even under extremely strong denaturing conditions (*31*, *36*).

The mobility of the spin-label in this position was very low at 20 °C. However, the faint but notable isotropic three-line features of the EPR spectra were more prominent in the presence of GroEL at 20 °C (Figure 6). Therefore, the substructure embracing the spin-label at position 97 seems to loosen up when GroEL interacts with the spin-W97C mutant. Proof that GroEL interacts with the spin-W97C mutant at 20 °C and thereby affects the conformation is provided by the following data: the enzyme exhibited only

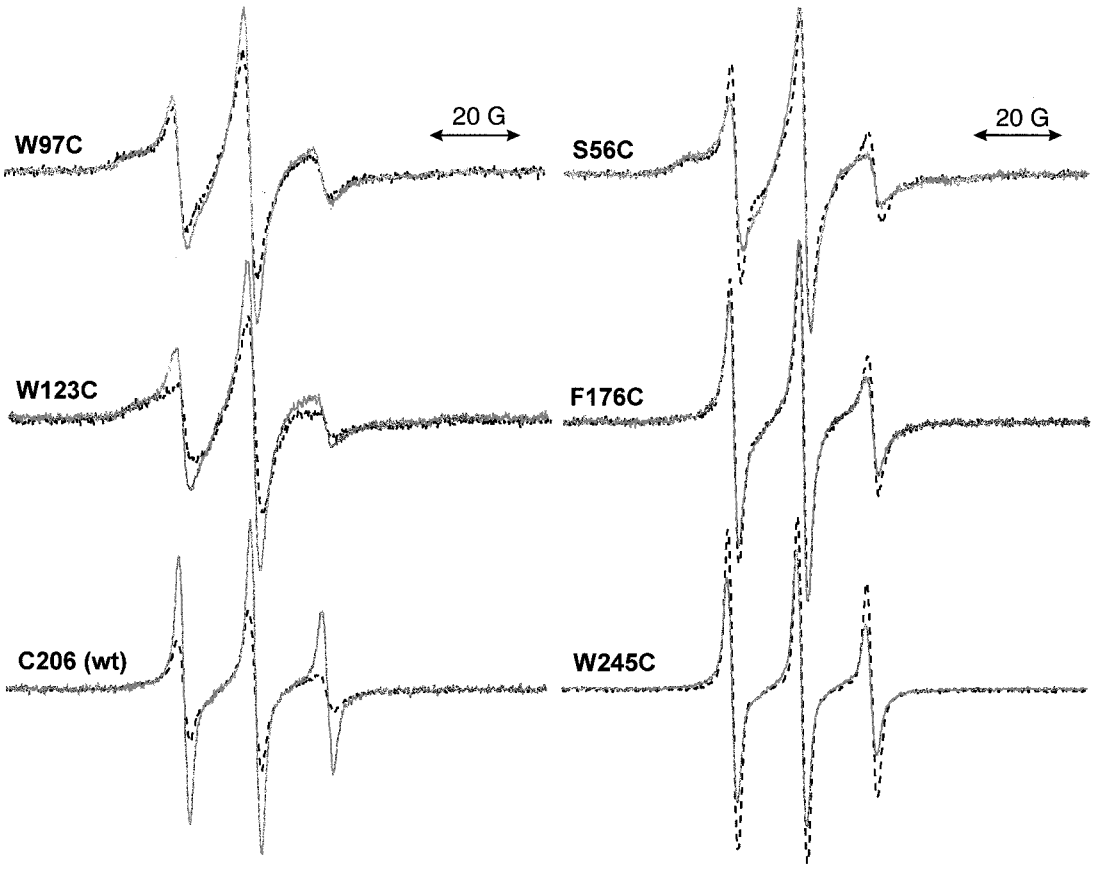


FIGURE 7: Various EPR spectra of spin-labeled variants of HCA II (indicated by insets) with (gray spectra) and without (dashed spectra) the presence of GroEL. All spectra were recorded at 50 °C, 5 min after the associated sample reached the incubation temperature. The spectra of samples with GroEL were all essentially unchanged during 1 h of heat treatment, whereas the EPR lines of samples without GroEL became broadened with time in a similar way as illustrated for spin-S56C in Figure 4. The time-dependent process for the variants without GroEL, together with the problem of instantly reaching the temperature within the sample (see Material and Methods), shows that the line-shape of the EPR spectra of the samples without GroEL should be regarded as slightly narrower if extrapolated to zero-time. The amplitude scale within each pair of normalized spectra is the same; however, the amplitude scale may differ among the various variants.

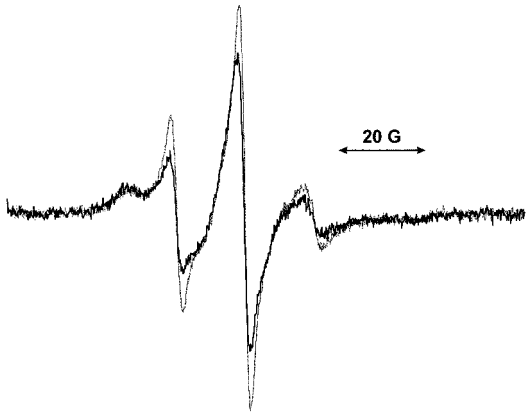


FIGURE 8: Effect of time on the EPR signal of spin-S56C during reactivation. The protein was heat-denatured at 50 °C in the presence of GroEL for 1 h, and reactivation was initiated by cooling to 20 °C. Both spectra were recorded with the sample at 20 °C: gray spectrum, recorded directly after the initiation of reactivation; black spectrum, recorded after 2 h of reactivation after heat treatment.

40% activity when GroEL was present, as compared to 85% in the absence of GroEL (Table 1).

As for all spin-HCA II variants without GroEL, increasing the temperature also increased the mobility of the spin-label, due to greater flexibility of the protein. However, the spin-label at 50 °C in position 97 was slightly more mobile in the presence than in the absence of GroEL (Figure 7).

*W123C*. Trp123 is located in $\beta$-strand 5, close to the surface of the protein (Figure 1). Data from chemical labeling experiments have shown that the region around position 123 is relatively rigid (*36*). At 20 °C there was no difference between the EPR spectra of spin-W123C obtained in the presence and the absence GroEL (Figure 6). The spin label appeared to be rather immobilized in both cases.

A difference between the two samples could be seen after the temperature was increased to 50 °C: the mobility of the spin-label in spin-W123C was greater in the presence than in the absence of GroEL (Figure 7). That means that GroEL makes the spin-label more mobile, which could be interpreted in the same way as for the spin-W97C mutant, that is, that GroEL induces conformational changes at the position of the spin-label. The structural change results in a more flexible surrounding at this position.

*C206*. Cys206 is located near the edge of $\beta$-strand 7. That $\beta$-strand and the vicinal sixth strand represent the most hydrophobic parts of the HCA II molecule (*48*). Cys206 is also near the active site of HCA II (Figure 1). Earlier studies have revealed that the native structure around this position is rather compact; that was indicated by low mobility of the spin-label (*31*).

EPR spectra of spin-C206 at 20 °C are shown in Figure 6. When comparing the spectra for spin-C206 at 20 °C with and without GroEL, it can be noted that the mobility of the

spin-label was somewhat larger when the chaperonin was present. That signifies that the structure around the spin-label in C206 becomes more flexible when GroEL is present. When the temperature was raised to 50 °C, the mobility of the spin-label increased in both samples (Figure 7). However, at that high temperature, the spin label in the sample with spin-C206 and GroEL was significantly more mobile than the spin label in the sample with spin-C206 alone.

In conclusion, the structure at the spin-label position becomes more flexible in the presence of GroEL at both 20 and 50 °C. Thus, similar effects of the GroEL interaction are observed for the spin-label in this position as when attached to positions 97 and 123.

*Interaction with Peripheral Positions*

*F176C*. Phe176 is located near the surface close to $\beta$-strand 1, and it is almost completely buried because its side chain points toward the interior of the molecule (Figure 1).

At 20 °C, no differences were observed in the EPR spectra of spin-F176C in the presence or absence of GroEL (Figure 6). In a sense, the mobility of the spin-label was intermediate between an immobilized (as in spin-C206, spin-W97C, and spin-W123C) and a mobile status (as in spin-W16C) (*29*, *31*).

After increasing the temperature to 50 °C, we saw a minor difference between the two samples: the surroundings of the spin-label were more rigid in the presence of GroEL (Figure 7). That implies that GroEL interacts with HCA II at position 176. However, the mobility of the spin-label was greater at 50 °C in the presence of GroEL than at 20 °C in the absence of the chaperonin, which is due to the temperature increase.

*W245C*. Trp245 is accommodated in a long loop between the central $\beta$-core and the N-terminal domain (Figure 1). At 20 °C, the equilibrium between the native state and the inactive intermediate of the spin-W245C mutant was hardly influenced by the presence of GroEL (Table 1). This is also in agreement with the corresponding EPR spectra recorded with and without GroEL, which do not show any significant spectral differences (Figure 6).

When the temperature was raised to 50 °C, the mobility of the spin-label increased both in the presence and in the absence of GroEL as noted above due to an increase in thermal energy. More important, however, is that the EPR spectrum of the spin-W245C sample with added GroEL indicates lower mobility of the spin-label than the spectrum of spin-W245C without GroEL (Figure 7). This suggests that an interaction also occurs between GroEL and HCA II at this position.

*Mapping the GroEL Interaction*. We have previously shown that GroEL interacted rather weakly with HCA II during the folding process at room temperature, and this was also true in the absence of GroES and ATP. The native conformation of HCA II was not affected by GroEL at that temperature. However, at elevated temperatures the interaction between GroEL and HCA II was shown to become stronger. It seemed as though the binding to GroEL caused a shift in the equilibrium toward an unfolded inactive intermediate that was in equilibrium with the native state. Although this intermediate was inactive, most of the activity was recovered after cooling. In the absence of the chaperonin very little enzyme activity was regained.

Table 2: Summary of Mobililty Changes of Spin-Probes upon Interaction

| HCA II variant | mobility at 20 °C without GrolEL | mobility at 50 °C with GroEL[a] |
|---|---|---|
| W97C | rigid | more mobile |
| W123C | rigid | more mobile |
| C206 (wt) | rigid | more mobile |
| W16C | mobile | more rigid |
| S56C | intermediate mobile | more rigid |
| F176C | mobile | more rigid |
| W245C | rigid/mobile | more rigid |

[a] Compared with HCA II variant alone.

Considering the present results regarding inactivation and reactivation in combination with the intrinsic fluorescence properties of the heat-inactivated spin-labeled HCA II variants, it seems that HCA II must assume a partially unfolded, molten globule-like conformation to be able to bind to GroEL.

Further, the decrease in $T_m$ (7 °C) for HCA II in the presence of GroEL indicates that the interaction with GroEL destabilizes the protein structure. This suggests that GroEL actively unfolds HCA II. A similar observation was made for the interaction of GroEL with barnase. In that case $T_m$ was decreased by 9 °C and it was concluded that GroEL catalyzes unfolding of bound proteins by using binding energy (*25*).

The structural changes that occur upon binding to GroEL are characterized in some detail by monitoring the mobility changes of the attached spin-labels (see Table 2 for a summary).

The spin-probes that were linked to peripheral positions of HCA II showed substantial mobility in the absence of GroEL but were all, to varying degrees, immobilized during interaction with GroEL. The other category of spin-labels that was attached to interior parts of the HCA II molecule was all largely immobilized in the absence of GroEL, even at elevated temperatures. Contrary to the surface-located spin-labels, these interiorly bound spin-labels became less immobilized during interaction with GroEL. It is important to note that the surface-located spin-labels during interaction with GroEL are still fairly mobile, whereas the movements of the mobilized interiorly located spin-labels are much more restricted. Therefore, it appears that the interior hydrophobic core still exists during interaction with GroEL. Nevertheless, considering the increased mobility of the spin-labels, it seems that the interaction with the chaperonin results in a more dynamic central core structure.

The motion of the spin-labels that are near or on the surface, on the other hand, becomes more constrained during the HCA II−GroEL encounter. It is not possible to deduce a detailed structure or the distance between the spin-label and GroEL from the EPR line-shape data. Since the line-shape of the spin-label in all positions when interacting with GroEL is far from the "rigid limit" associated with the size of HCA II (compared with data for the native W97C case (*31*)), the dynamic signature dominating the EPR spectrum is the local motions of the spin-labeled side chain. Hence, a pronounced effect on the rotational diffusion due to the large

molecular weight of GroEL, even in close contact to the substrate protein, is not expected.

Another possible scenario is that GroEL causes a general disorder in the molecular structure of HCA II. This interpretation of the our data is, however, less plausible because interaction with GroEL resulted in two different types of mobility changes of the spin-labels depending on the location of the spin-labels in the native state of HCA II. In addition, these two categories of spin-labels differed significantly in regard to their final mobility, which shows that the spin-label environments still are remarkably different in the GroEL-bound state.

Earlier characterizations of folding intermediates of HCA II have shown that the protein can adopt a stable and compact equilibrium folding intermediate conformation of molten-globule-type (*31*, *36*). The predominant $\beta$-structure, which consists of 10 $\beta$-strands that extend throughout the entire molecule, appears to be largely intact in this intermediate. However, the outermost $\beta$-strands were found to be flexible and less stable than the interiorly located $\beta$-strands, showing that the outer parts of the structure are more labile. Of the positions probed only those exposed in the molten-globule (positions 16, 56, 176, 245) had spin-probes that were immobilized during interaction with GroEL. This part of the EPR data indicates that the bound intermediate of HCA II is unfolded at least to the same extent as the molten-globule intermediate. Specifically, the outer part of the main domain $\beta$-core (probed at positions 56 and 176) seems to interact with GroEL. This appears also to be the case for the minor N-terminal domain (position 16) and the interface between the two domains (position 245).

We have previously reported that a hydrophobic region, containing $\beta$-strands 3−5, seems to be remarkably stable and is not ruptured until extremely strong denaturing conditions (approximately 5 M GuHCl) are applied (*31*, *36*). In a recent study, we demonstrated that $\beta$-strands 6 and 7 are also included in this stable residual structure (*37*). That this compactness is retained after heat denaturation is also demonstrated by our present data showing broad line-widths in the EPR spectra of the spin-labels in this area of the molecule (positions 97, 123, and 206; Figure 7). It was noted that the spin-labels were somewhat more mobile in this region when GroEL was present, which indicates that the structure of the hydrophobic core becomes more flexible than in the corresponding unchaperoned state. By making the rigid core structure more dynamic GroEL will facilitate rearrangements of misfolded structure. From this observation it is clear that GroEL can participate actively in the folding process by loosening up structural elements. In regard to HCA II such an active role for GroEL is supported by our previous finding that the apparent activation energy for reactivation of the denatured enzyme is lowered by GroEL, which strongly indicates that GroEL influences the folding pathway (*28*).

*Nonspecific Hydrophobic Interactions between GroEL and HCA II*. The observed relationship between the binding of HCA II to GroEL and the stability of the enzyme (Figure 3) shows that the insertion of the spin-label has little or no direct effect on the affinity for GroEL. In 5 of the 6 mutants, aromatic residues (4 Trp and 1 Phe) had been substituted, leading to uniform alterations in the local structure in the spin-labeled positions. That implies that the degree of binding to GroEL is dependent on the stability of the HCA II variant: that is, the easier the molten-globule-like intermediate can be formed, the more of the protein substrate will be captured by GroEL. This observation supports the idea that nonspecific hydrophobic interactions are most important for formation of the GroEL−substrate complex (*11*−*19*).

*The Conformation of Bound Protein Substrates*. How much of the native conformation that is present in a protein substrate complexed to GroEL is a question that lacks an unequivocal answer and is therefore still a subject of discussion. In some cases it has been proposed that GroEL-bound proteins are completely unfolded. Other studies suggest that the protein substrates are partially structured and that many of them have structural features that resemble a molten-globule-like conformation, that is, they have a significant amount of nativelike secondary structure but no stable tertiary interactions and they have exposed hydrophobic patches. It has also been reported that the properties of the bound protein are similar to those of the native state (*4*). It has also been shown that in some cases binding of GroEL leads to further unfolding of the substrate (*16*, *23*−*25*).

Evidently, the conformational state recognized by GroEL is not unique. Our data suggest that the formation of a protein−substrate complex depends on the thermodynamic stability and that this influences the partitioning between the bound and unbound protein substrate. The hydrophobic core of the molten-globule state of HCA II has been shown to be extremely stable (*31*, *36*), and that is probably the reason GroEL is not capable of fully unfolding the polypeptide chain. Apparently, it seems as though the degree of unfolding of protein substrates depends on the stability and size of the hydrophobic core.

*Concluding Remarks*. The main conclusions that can be drawn from this study are the following: (i) HCA II needs to be unfolded to a degree similar to that of a GuHCl-induced molten-globule intermediate of the enzyme for the initial interaction with GroEL to take place; (ii) the degree of binding to GroEL depends on the stability of the HCA II variant; (iii) GroEL efficiently protects HCA II from irreversible aggregation at higher temperatures; (iv) interaction with GroEL leads to higher flexibility of the rigid and compact hydrophobic core of HCA II, which is likely to facilitate rearrangements of misfolded structure; (v) the secondary structure of the bound intermediate is not known but it is clear that the protein becomes more flexible upon binding than the well-characterized molten-globule state; (vi) protein−protein interactions can be specifically mapped by site-directed spin-labeling and EPR measurements.

## ACKNOWLEDGMENT

We are very much indebted to Dr. Anthony Gatenby, E. I. DuPont de Nemours and Company, for kindly providing pT7GroE plasmid. We also wish to thank Dr. Nils Bergenhem, Novo Nordisk A/S, for discussions of the manuscript.

## REFERENCES

1. Laskey, R. A., Honda, B. M., Mills, A. D., and Finch, J. T. (1978) *Nature 275*, 416−420.
2. Hartl, F. U. (1996) *Nature 381*, 571−580.
3. Thomas, J. G., Ayling, A., and Baneyx, F. (1997) *Appl. Biochem. Biotechnol. 66*, 197−238.

4. Fenton, W. A., and Horwich, A. L. (1997) *Protein Sci. 6*, 743−760.
5. Horovitz, A. (1998) *Curr. Opin. Struct. Biol. 8*, 93−100.
6. Ellis, R. J. (1996) *Folding Des. 1*, R1−R15.
7. Burston, S. G., Sleigh, R., Halsall, D. J., Smith, C. J., Holbrook, J. J., and Clarke, A. R. (1992) *Ann. N. Y. Acad. Sci. 672*, 1−9.
8. Braig, K., Otwinowski, Z., Hegde, R., Boisvert, D. C., Joachimiak, A., Horwich, A. L., and Sigler, P. B. (1994) *Nature 371*, 578−586.
9. Boisvert, D. C., Wang, J., Otwinowski, Z., Horwich, A. L., and Sigler, P. B. (1996) *Nat. Struct. Biol. 3*, 170−177.
10. Xu, Z., Horwich, A. L., and Sigler, P. B. (1997) *Nature 388*, 741−750.
11. Fenton, W. A., Kashi, Y., Furtak, K., and Horwich, A. L. (1994) *Nature 371*, 614−619.
12. Buckle, A. M., Zahn, R., and Fersht, A. L. (1997) *Proc. Natl. Acad. Sci. U.S.A. 94*, 3571−3575.
13. Hayer-Hartl, M. K., Ewbank, J. J., Creighton, T. E., and Hartl, F. U. (1994) *EMBO J. 13*, 3192−3102.
14. Zahn, R., Axmann, S. E., Rücknagel, K.-P., Jaeger, E., Laminet, A. A., and Plückthun, A. (1994) *J. Mol. Biol. 242*, 150−164.
15. Zahn, R., and Plückthun, A. (1994) *J. Mol. Biol. 242*, 165−174.
16. Itzhaki, L., Otzen, D., and Fersht, A. L. (1995) *Biochemistry 34*, 14581−14587.
17. Lin, Z., Schwartz, F. P., and Eisenstein, E. (1995) *J. Biol. Chem. 270*, 1011−1014.
18. Katsumata, K., Okazaki, A., Tsurupa, G. P., and Kuwajima, K. (1996) *J. Mol. Biol. 264*, 643−649.
19. Sparrer, H., Lilie, H., and Buchner, J. (1996) *J. Mol. Biol. 258*, 74−87.
20. Aoki, K., Taguchi, H., Shindo, Y., Yoshida, M., Ogasahara, K., Yutani, K., and Tanaka, N. (1997) *J. Biol. Chem. 272*, 32158−32162.
21. Dessauer, C. W., and Bartlett, S. G. (1994) *J. Biol. Chem. 269*, 19766−19776.
22. Perrett, S., Zahn, R., Stenberg, G., and Fersht, A. L. (1997) *J. Mol. Biol. 269*, 892−901.
23. Zahn, R., Spitzfaden, C., Ottiger, M., Wüthrich, K., and Plückthun, A. (1994) *Nature 368*, 261−265.
24. Walter, S., Lorimer, G. H., and Schmid, F. X. (1996) *Proc. Natl. Acad. Sci. U.S.A. 93*, 9425−9430.
25. Zahn, R., Perret, S., and Fersht, A. R. (1996) *J. Mol. Biol. 261*, 43−61.
26. Persson, M., Aronsson, G., Bergenhem, N., Freskgård, P.-O., Jonsson, B.-H., Surin, B. P., Spangfort, M. D., and Carlsson, U. (1995) *Biochim. Biophys. Acta 1247*, 195−200.
27. Persson, M., Carlsson, U., and Bergenhem, N. (1997) *FEBS Lett.* 411, 43−47.
28. Persson, M., Bergenhem, N., and Carlsson, U. (1996) *Biochim. Biophys. Acta 1298*, 191−198.
29. Lindgren, M., Svensson, M., Freskgård, P.-O., Carlsson, U., Jonsson, B.-H., Mårtensson, L.-G., and Jonasson, P. (1993) *J. Chem. Soc., Perkin Trans. 2*, 2003−2007.
30. Lindgren, M., Svensson, M., Freskgård, P.-O., Carlsson, U., Jonasson, P., Mårtensson, L.-G., and Jonsson, B. H. (1995) *Biophys. J. 69*, 202−213.
31. Svensson, M., Jonasson, P., Freskgård, P.-O., Jonsson, B.-H., Lindgren, M., Mårtensson, L.-G., Gentile, M., Borén, K., and Carlsson, U. (1995) *Biochemistry 34*, 8606−8620.
32. Farahbakhsh, Z. T., Huang, Q.-L., Ding, L.-L., Altenbach, C., Steinhoff, H.-J., Horwitz, J., and Hubbel, W. L. (1995) *Biochemistry 34*, 509−516.
33. Eriksson, A. E., Jones, T. A., and Liljas, A. (1988) *Proteins: Struct., Funct., Genet. 4*, 274−282.
34. Håkansson, K., Carlsson, M., Svensson, L. A., and Liljas, A. (1992) *J. Mol. Biol. 277*, 1192−1204.
35. Carlsson, U., and Jonsson, B.-H. (1995) *Curr. Opin. Struct. Biol. 5*, 482−487.
36. Mårtensson, L.-G., Jonsson, B.-H., Freskgård, P.-O., Kihlgren, A., Svensson, M., and Carlsson, U. (1993) *Biochemistry 32*, 224−231.
37. Hammarström, P., Kalman, B., Jonsson, B.-H., and Carlsson, U. (1997) *FEBS Lett. 420*, 63−68.
38. Mizobata, T., and Kawata, Y. (1994) *Biochim. Biophys. Acta 1209*, 83−88.
39. Sparrer, H., Lilie, H., and Buchner, J. (1996) *J. Mol. Biol. 258*, 74−87.
40. Hemmingsen, S. M., Woolford, C., van der Vies, S. M., Tilly, K., Dennis, D. T., Georgopoulos, C. P., Hendrix, R. W., and Ellis, R. J. (1988) *Nature 333*, 330−334.
41. Bradford, M. (1976) *Anal. Biochem. 72*, 248−254.
42. Rickli, E. E., Ghazanfar, S. A. S., Gibbons, B. H., and Edsall, J. T. (1964) *J. Biol. Chem. 239*, 1065−1078.
43. Freskgård, P.-O., Bergenhem, N., Jonsson, B.-H., Svensson, M., and Carlsson, U. (1992) *Science 258*, 466−468.
44. Pace, C. N., and Scholtz, J. M. (1997) in *Protein Structure. A Practical Approach.* (Creighton, T. E., Ed.) pp 299−321, Oxford University Press, Oxford, U.K.
45. Mårtensson, L.-G., Jonasson, P., Freskgård, P.-O., Svensson, M., Carlsson, U., and Jonsson, B.-H. (1995) *Biochemistry 34*, 1011−1021.
46. Mårtensson, L.-G., Ph.D. (1993)Thesis ISBN 91-7174-842-3 University of Umeå, Umeå, Sweden.
47. Todd, M. J., and Lorimer, G. H. (1995) *J. Biol. Chem. 270*, 5388−5394.
48. Bergenhem, N., Carlsson, U., and Karlsson, J.-Å. (1989) *Int. J. Pept. Protein Res. 33*, 140−145.


BI981442E